A Study of Velocity Profiles Through the Main Thermocline[1]

H. THOMAS ROSSBY

Graduate School of Oceanography, University of Rhode Island, Kingston 02881

THOMAS B. SANFORD

Woods Hole Oceanographic Institution, Woods Hole, Mass. 02543

(Manuscript received 23 February 1976, in revised form 20 May 1976)

ABSTRACT

A time series of velocity profiles derived from three methods are used to describe the variations of current in time and in the vertical. Absolute velocity profiles were obtained by acoustically tracking a falling probe; relative profiles were derived from motional electric fields (EM method) measured by a second free-fall instrument and from density observations using the dynamic method. The two free-fall profile methods agree within 0.01 m s^{-1} rms averaged over depth intervals in which the observations were separated in time by less than 10 min. Although the rms differences between profiles increases to about 0.02 m s^{-1}, due to the fact that one device falls at one-third the speed of the other, the agreement between methods was sufficiently good that the eight acoustic profiles and six EM profiles were combined to yield a time series lasting 4 days. These profiles, taken near Bermuda in May 1971, were divided into two sets having a mean time separation of 2 days. Each set of profiles was fitted to a time-mean or steady profile and a rotary component of inertial frequency. Using lagged correlation and vector spectral analysis, it is shown that the inertial energy propagates downward at a group velocity having a vertical component of about 0.5 mm s^{-1}. These results suggest a surface or near-surface energy source and a lack of modal structure to the inertial currents. The steady component agrees within 0.02 m s^{-1} rms with the geostrophic profile computed every 200 m and both have the same shear over the interval 200–1200 m.

1. Introduction

Velocity profile observations have revealed considerable complexity to the vertical structure or distribution of currents in the deep sea. Zones of enhanced variability are observed throughout the water column, but are most frequently found near the surface, within the main thermocline and within 500 m of the sea floor. An individual profile is composed of a superposition of a wide spectrum of different spatial and temporal scales of motion operating simultaneously.

In a previous study (Rossby, 1974) of low-frequency variability of the velocity profile at one site, it was evident that monthly or even weekly sampling was inadequate to follow the time evolution of the velocity profile. Low-frequency (quasi-geostrophic) structure can be advected past the observation site in a matter of days. Moreover, high-frequency contributions, such as due to internal tidal or inertial period motions, are important constituents to an individual profile. Repeated velocity profiles at one site are needed in order to estimate the energy contributed by a variety of time-dependent motions.

This paper interprets a time series of observations from three different velocity profile methods. Rossby applied a velocity profile method (Rossby, 1969) based on acoustically tracking a free-fall probe. Simultaneously, Sanford utilized a free-fall velocity profiler (Drever and Sanford, 1970) based on the principles of motional induction (EM method). Each profile method has been used extensively in the field with little evaluation of performance. Each method is based on different principles of operation and each is susceptible to different sources of error. This experiment was the first opportunity for the two free-fall methods to be operated simultaneously. In addition, a third profile method, the classical dynamic method for determining the vertical shear of geostrophic currents by the thermal wind relation, is compared with the two profiler methods.

We seek to chart, if only crudely, the joint frequency-vertical wavenumber distribution of kinetic energy. With the time series available it is possible to describe the composition of the vertical structure in three frequency bands: a steady or geostrophic component, an inertial-frequency band and a lumped, high-frequency band. Much of the analysis in this paper concentrates on the inertial-frequency band motions. Theoretical studies of inertial motion (Munk and Phillips, 1968; Pollard, 1970) commonly assume a vertical structure given by a sum of vertical normal modes. The existence of normal modes is not supported by the present data. Rather it is found that kinetic energy propagates downward, perhaps as isolated

[1] W.H.O.I. Contribution No. 3712.

events or packets of energy. This result is consistent with energy production by winds (Pollard, 1970) and the low coherencies near the inertial frequency computed between vertically separated current meters (Webster, 1972; Siedler, 1971).

In summary, we examine two quite separate questions. The first concerns the consistency of three methods for determining the vertical structure and the other deals with the structure and evolution of the vertical profiles of horizontal motion over a period of a few days. We begin the study with a discussion of the operation and a comparison of the results of the free-fall profilers. The results agree sufficiently well that we have no hesitancy in combining the data into one set. Then, using all the profiles, we examine the structure of the current field in several ways and compare these results with the dynamically computed vertical shear.

2. The velocity profile methods

The acoustic method obtains a velocity profile from the acoustical determination of the trajectory of a freely falling probe. This method, using moored hydrophones, is more fully described elsewhere (Rossby, 1969, 1974). The trajectories in the vertical and east and the vertical and north planes during an interval of 200 s are separately fitted in a least-square sense to parabolic curves. The fitted curve is differentiated with respect to time to determine the east, north and vertical velocity components of the probe's motion. It is assumed that the horizontal velocity components of the float are equal to those of the surrounding water. The rms difference between the measured and fitted trajectories is typically 1 m. Thus, if the instrument is sinking at 0.25 m s^{-1} in the presence of a 0.10 m s^{-1} horizontal current it will be advected 20 m horizontally during a 50 m vertical interval. A single endpoint determination of the advection rate without any curve fitting would lead to a maximum 10% or 0.01 m s^{-1} uncertainty in horizontal speed. The least-square curve fit reduces this level of expected error.

The EM profile data were obtained from a free-fall instrument operating on the principle of geomagnetic induction. The instrument, described by Drever and Sanford (1970), measures the voltages induced by the motion of the sea and instrument through the geomagnetic field. The electric field is interpreted in terms of velocity according to the relations given by Sanford (1971).

As the probe freely falls toward the bottom, the voltages sensed across two electrodes, 1 m apart horizontally, are measured and acoustically telemetered to the ship. Additionally, pressure, temperature and the orientation of the electrode line relative to magnetic north are telemetered and recorded in real-time. The horizontal electric field is determined from the measured voltages and orientation. The contribution to the electric field from the fallspeed ($\sim$1 m s^{-1}) is

TABLE 1. Vertically averaged horizontal velocities and kinetic energies for the eight acoustical (AC) and six electromagnetic (EM) profiles averaged between 100–1000 m and 100–1500 m depths. The suffix D or U added to the profile number denotes whether the down or up traverse is used. The time given is for the start of acoustical and down EM profiles or is the end (surface time) of an up EM profile. The times are relative to 0000 26 May 1971.

Profile number	1	2	3	4	5	6	7	8	69D	70D	71U	73U	75D	76D
Profiler type	AC	AC	AC	AC	AC	AC	AC	AC	EM	EM	EM	EM	EM	EM
Time (h)	4.1	22.5	28.8	42.5	46.9	72.7	91.6	105.5	4.5	23.0	30.5	43.4	91.8	105.8
$\bar{u}$ (m s^{-1})	−0.051	−0.041	−0.067	−0.040	−0.048	−0.054	−0.052	−0.033	−0.047	−0.037	−0.063	−0.043	−0.052	−0.033
$\bar{v}_{100-1000\ m}$	0	0.039	0.042	0.053	0.080	0.083	0.048	0.046	0.017	0.036	0.048	0.056	0.050	0.045
$\overline{K.E.}$ (J m^{-3})	2.06	2.79	4.20	3.41	5.36	6.02	3.65	2.12	1.85	2.60	4.17	4.24	3.99	2.60
$\bar{u}$ (m s^{-1})	−0.047	−0.036	−0.064	−0.032	−0.039	−0.047	−0.046	−0.032	−0.047	−0.036	−0.063	—	—	—
$\bar{v}_{100-1500\ m}$	0.018	0.022	0.031	0.046	0.050	0.049	0.043	0.045	0.015	0.023	0.031	—	—	—
$\overline{K.E.}$ (J m^{-3})	2.04	2.07	3.41	2.53	3.70	4.20	3.05	1.99	1.72	1.93	3.53	—	—	—
Maximum depth (m)	1710	1515	1705	1675	1660	1660	1610	1705	2000	2000	2000	1100	1100	1000
Fallspeed (m s^{-1})	−0.27	−0.27	−0.28	−0.28	−0.28	−0.28	−0.28	−0.28	−0.87	−0.87	0.72	0.72	−0.90	−0.90

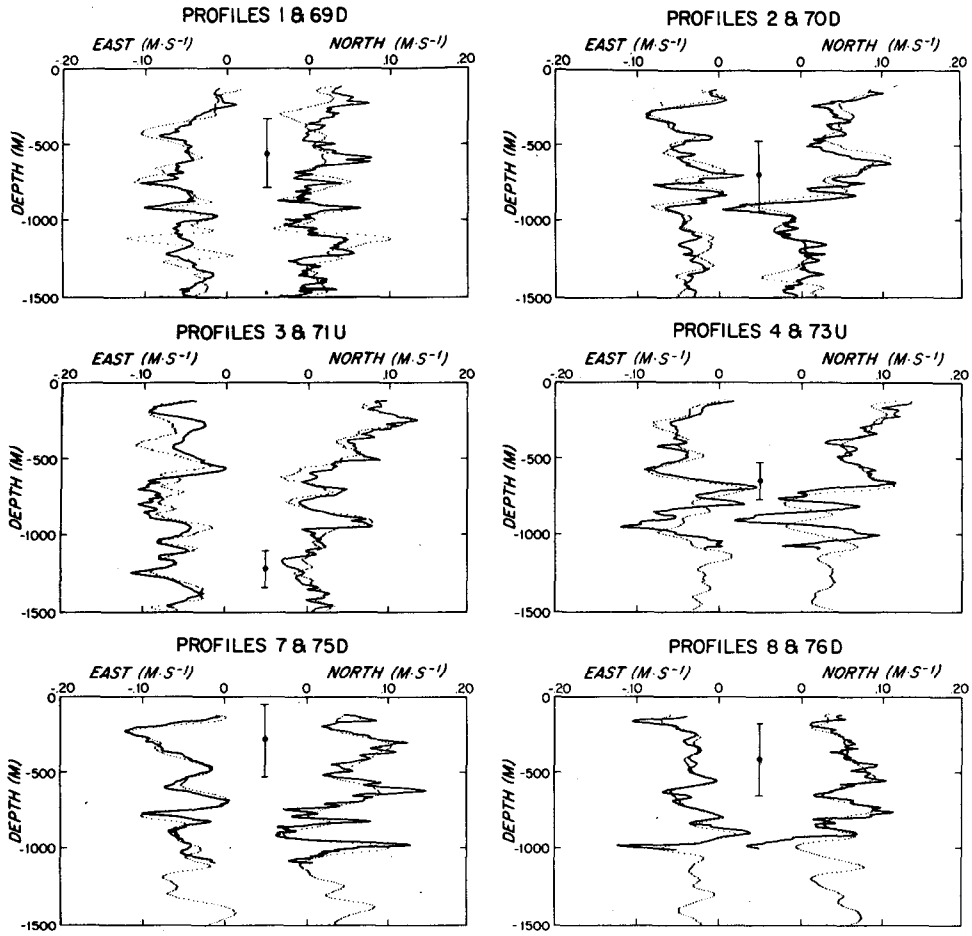

FIG. 1. Profiles of velocity components obtained by Rossby (dotted lines) and Sanford (solid lines). The solid circles indicate depths simultaneously reached by both instruments. The vertical lines from the solid circle indicate the range of depths over which the two profiles were observed within a time separation of ± 10 min. The suffixes D or U denote that data presented are from down or up traverses of the EM profiler.

removed during analysis using the rate of change of pressure.

These telemetered data, recorded in analog form on a graphical recorder (PGR), are digitized to yield values of electric field (amplitude and direction), temperature, pressure and fall rate every 7–8 m. Linear interpolation is used to obtain profile values every 5 m. Fall rate and direction values are smoothed by an 11-point, triangularly tapered filter. The resulting profiles have a vertical resolution of about 20 m. Even after averaging, the fall rate determination is noisy, producing about ± 0.01 m s^{-1} small-scale variability in the north component profiles. The electric field is converted to equivalent velocity. This conversion yields a velocity profile which is relative to an unknown constant, independent of depth.

3. The experiment and profiler intercomparison

The experiment consisted of a series of velocity profiles taken between 26 and 30 May 1971 at a site 4500 m deep located 90 km south of Bermuda. The weather was fair with ESE winds at 5–8 m s^{-1} and changing to SSE at 7–10 m s^{-1} by the end of the 5-day period. We attempted to commence the profiles at the same location, but due to winds and inadequate navigation the starting point varied considerably. Nonetheless, the two profilers were launched within 1 km horizontally. Toward the end of the cruise, the starting points were closer (200–300 m) and within 15 min in time. After a few trials it became our practice to drop the acoustic profiler first (because of its slower descent rate) and then the EM profiler, with the recovery in reverse order.

In Table 1 we summarize the starting conditions for all the drops and the vertically-averaged velocities between 100 and 1000 m. The motion is more energetic above and within the main thermocline than below. That is, the vertically-averaged kinetic energy of each profile in Table 1 is larger over the interval 100–1000 m than over the span 100–1500 m. Also the fluctuations in energy level from profile to profile indicate that a significant portion of the vertically-averaged kinetic

energy is time-dependent. It should be stressed that the averages shown for the EM profiles are not measured but are obtained after comparison with the acoustic profiles. The addition of a depth-independent contribution is necessitated by the fact that the EM profiler cannot determine the barotropic component of motion. As we show below, the techniques compare sufficiently well in every other regard that we have added the barotropic component as determined from the acoustic profiler.

Fig. 1 present the profile pairs which have sections of nearly simultaneous data. The acoustic profiler is tracked only during its descent, while the EM profiler operates on both the down (D) and up (U) traverses. Since the two profilers fall (or rise) at different speeds, there are at most two depths at which simultaneous current measurements are obtained; the first depth of coincidence occurs during the descent of the EM probe and the second is encountered in its ascent. The vertical bars on Fig. 1 indicate the interval samples by the two instruments within a time difference of ± 10 min.

Much variability in time and depth is evident in the six profile pairs of Fig. 1. Frequently the current is observed to change by 0.10–0.15 m s^{-1} over 10 h between profiles or over 100 m on a single profile. The fluctuations are sufficiently strong that the time mean velocity profile is not strongly revealed.

Several of the important sources for discrepancies between the two methods are evident in Fig. 1: nonsimultaneity of measurements at all depths, errors in the measurement of depth between profilers, different vertical resolution and data averaging, and errors in the north component of EM profiles due to uncertainties in fall rate corrections.

In general, the agreement between the methods is best over the data segments which are close in time, say within 10 min. Over the 10 min segments the profiles differ by about 0.01–0.02 m s^{-1} rms. With few exceptions, both methods observe the same vertical structure. The principal exceptions to this rule occur between 1000 and 1200 m on profiles 1 and 69D and below 700 m on profiles 4 and 73U. The cause of the differences between 1 and 69D is not known, while 4 and 73U are different because of a systematic depth error evident below 700 m. The rms difference observed over the six profile pairs between 100–1000 m is 0.024 m s^{-1}.

The last two profile pairs were obtained at a time when the profilers were launched closely in time and space and the acoustic signals used by both methods were clearly received. Over the ± 10 min interval, the standard deviations between 7 and 75D and between 8 and 76D are about 0.01 m s^{-1}, while over the interval 100–1000 m the standard deviations increase to about 0.03 m s^{-1}.

In summary, we find that the two methods yield identical profiles to within ± 0.01 m s^{-1} rms when launched together and when the acoustic signals are well resolved. Also some of the error arises due to systematic errors in depth (pressure) measurements, an error source which can be eliminated by improved design. Considering all of the profile pairs, uncertainties of less than 0.02 m s^{-1} rms were observed over the ± 10 min regions.

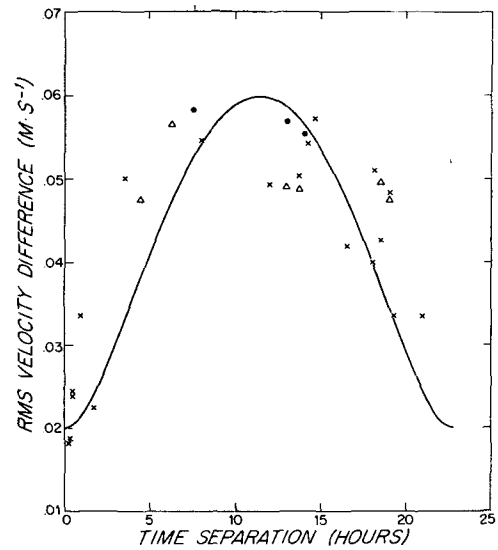

FIG. 2. The rms velocity differences between profiles separated in time. Symbols denote velocity differences as derived from pairs of acoustic profiles (△), from pairs of electromagnetic profiles (●) and from acoustic-EM pairs (×). The solid line represents a fit of inertial motion model to the data [see Eq. (2)].

4. The temporal variability of the profile series

For larger time separations between profiles, it is possible to examine the behavior of differences between profiles of the same as well as between different methods. Fig. 2 presents profile differences as a function of time separation, where the rms difference is computed as

$$D(t_2-t_1)=\tfrac{1}{2}\overline{[(u_2-u_1)^2+(v_2-v_1)^2]}^{\frac{1}{2}}, \qquad (1)$$

where u_1, v_1 are the east and north velocity components at depth z for profile taken at time t_1, and u_2, v_2 the east and north velocity components at depth z for profile taken at time t_2; the overbar represents an average over depth interval 100–1000 m.

As the time separation approaches 10–12 h, the rms velocity differences reach a peak value of about 0.06 m s^{-1}. Thus the variance of the differences is about an order of magnitude larger than for separations of less than an hour, which we take as our difference noise level. For time separations approaching the diurnal-inertial period (the inertial period is 22.8 h), the rms velocity differences tend to decrease toward values slightly larger than found for small time separations.

The general form of the difference data suggests that a major contribution to the time-dependent variance

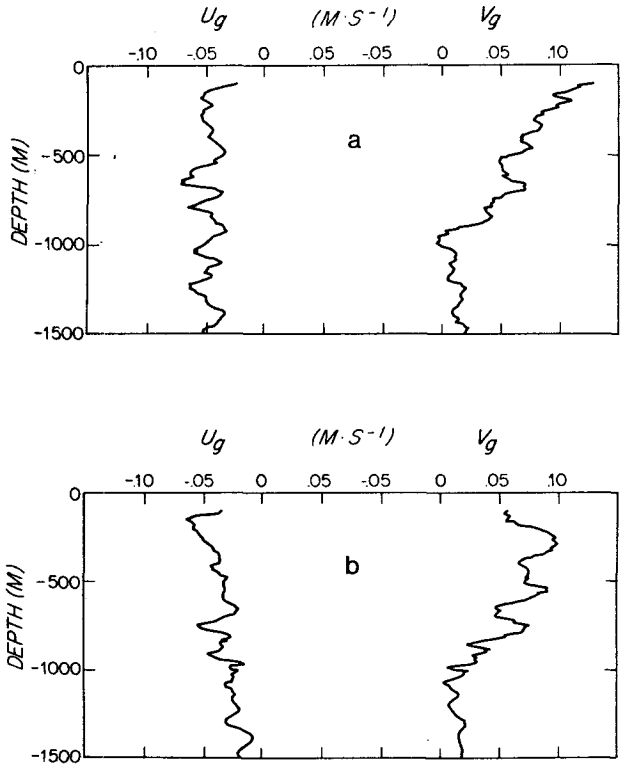

FIG. 3. Steady east (U_g) and north (V_g) velocity components as computed from Eq. (3) for sets 2-5 (a) and 5-8 (b).

results from inertial period motions. In Fig. 2 we compare the observed velocity differences with what would be expected if the time-dependent velocity variations were dominated by inertial currents plus observational noise. The solid curve in Fig. 2 represents the combined influences of motions of inertial period (22.8 h) having a vertically averaged amplitude (C) of 0.04 m s^{-1} plus the expected measurement noise (n) of 0.02 m s^{-1}, i.e.,

$$D(t_2-t_1)=[2C^2\sin^2\omega(t_2-t_1)/2+n^2]^{\frac{1}{2}}, \qquad (2)$$

where $\omega=(2\pi/22.8)$ h. The similarity between the data and the simple model suggests that a more refined model or decomposition of the near-inertial velocity data would be useful.

The data presented in Figs. 1 and 2 reveal no systematic differences between profiler methods. Therefore, the data from each method were combined into one data set for subsequent analysis.

To resolve more clearly the time- and depth-dependent fluctuations, the series of combined profiles was decomposed into the contributions from three frequency bands. The profile series was fitted at each depth level to the following four-parameter model:

$$\left.\begin{aligned} u(z,t)&=U_g(z)+A(z)\cos\omega t-B(z)\sin\omega t+u'(z,t)\\ v(z,t)&=V_g(z)-A(z)\sin\omega t-B(z)\cos\omega t+v'(z,t)\end{aligned}\right\}. \qquad (3)$$

We have computed the coefficients by a standard least-square procedure at each depth level using either all or various subsets of the profiles. The time-mean or steady components of motion are represented by U_g and V_g. The inertial period motion, which is estimated at a fit frequency (ω) 5% larger than f (typical of most spectra of inertial oscillations), is assumed to be circular and represented by a rotary current of amplitude and phase determined by the A and B coefficients

$$\left.\begin{aligned} A\cos\omega t-B\sin\omega t&=V_I\cos(\omega t+\Phi_I)\\ -A\sin\omega t-B\cos\omega t&=-V_I\sin(\omega t+\Phi_I)\end{aligned}\right\}. \qquad (4)$$

Hence

$$V_I=(A^2+B^2)^{\frac{1}{2}},\quad \Phi_I=\tan^{-1}B/A.$$

The high-frequency fluctuations represented by u' and v' are the velocity differences between the model and the data series.

The purposes of this model fit are 1) to reveal the composition of the vertical structure due to motion in three frequency bands and 2) to detect time evolution of the structure. For these reasons, we have separately fitted the model to profiles from the first and second halves of the 5-day series. The first series, denoted as series 2-5, is composed of profiles 2, 3, 4, 5, 70D and 71U, while the second series, denoted as series 5-8, consists of profiles 5, 6, 7, 8, 73U, 75D and 76D. The results of the two decompositions are presented in Figs. 3–5.

First, it is evident (Fig. 4) that many of the promi-

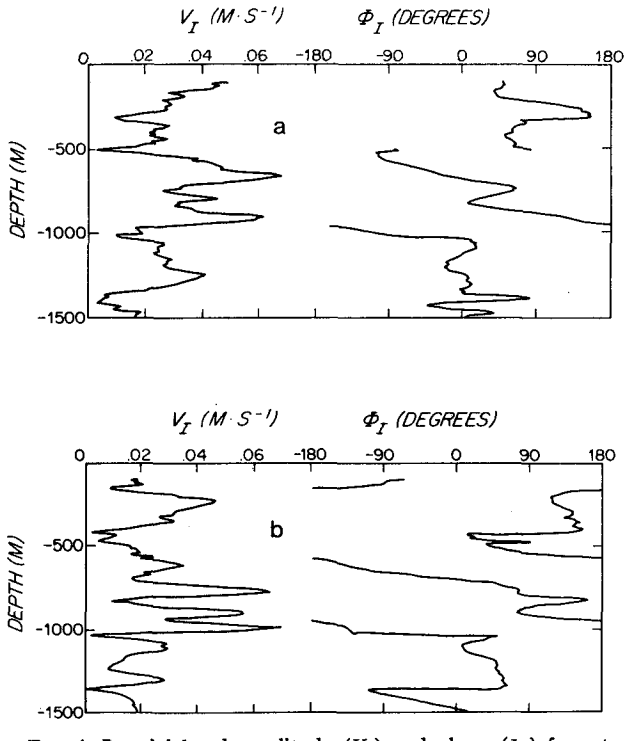

FIG. 4. Inertial band amplitude (V_I) and phase (Φ_I) for sets 2-5 (a) and 5-8 (b). Phase is computed relative to a reference time of 0000 GMT 26 May 1971.

nent features or peaks of V_I in the 2-5 series reappear later in the 5-8 series, but at slightly deeper depths. Second, whereas the amplitude fluctuates greatly with depth, the phase is more regular tending to increase with depth. Both the apparent vertical shift of amplitude with time and the phase advance with depth are consistent with the vertical propagation of inertial waves.

The variations of Φ_I in Fig. 4 are identical to the changes in the direction of the inertial current measured in the customary sense for current measurements (clockwise from north). Thus as Φ_I increases with depth, the inertial current rotates clockwise when the u, v hodograph is viewed from above.

The sense of rotation can be related to the direction of the vertical group velocity for an individual wave of inertial frequency (f). Consider a free wave of vertical wavenumber m

$$u+iv=Se^{i(mz-ft)},$$

where, since $z\leqslant 0$, the u, v hodograph rotates clockwise with depth for $m>0$. Also for $m>0$ the phase velocity of the wave is upward, while the vertical group velocity is downward. The group velocity is derived from the dispersion relation for free internal waves in a region of uniform N without mean current shear, i.e.,

$$\omega^2=\frac{k^2N^2+m^2f^2}{m^2+k^2},$$

where m and k are the vertical and horizontal wavenumbers. For $\omega=f(1+\epsilon)$, where $\epsilon\ll 1$ and for $m^2\gg k^2$, the vertical group velocity is approximately

$$C_g=\frac{\partial\omega}{\partial m}=-\frac{2f\epsilon}{m}. \tag{5}$$

From Fig. 4, it appears that $m\approx 2\pi/400$ m and is positive. Taking $f=8\times10^{-5}$ s^{-1} and $\epsilon=5\times10^{-2}$, we have

$$C_g=-0.5 \text{ mm s}^{-1}. \tag{6}$$

The correspondence between current rotation with depth and vertical group velocity is not unique when more free inertial waves of different vertical wavelengths are combined. In fact, even the sum of standing waves or modes can exhibit phase rotation, even though each mode individually has no direction change with depth nor net vertical energy flux. Thus in order to apply the group velocity analysis it is necessary to decompose the profile in terms of the contributions at each vertical wavenumber.

To investigate energy propagation further, the kinetic energies of the V_I profiles of Fig. 4 were formed and cross-correlated. It was found that the kinetic energy of the inertial band is most correlated from the first to the second sequence for a depth lag of 100 m. That a shift of 100 m achieves a high cross-correlation can be seen in Fig. 6 in which the kinetic energy of the

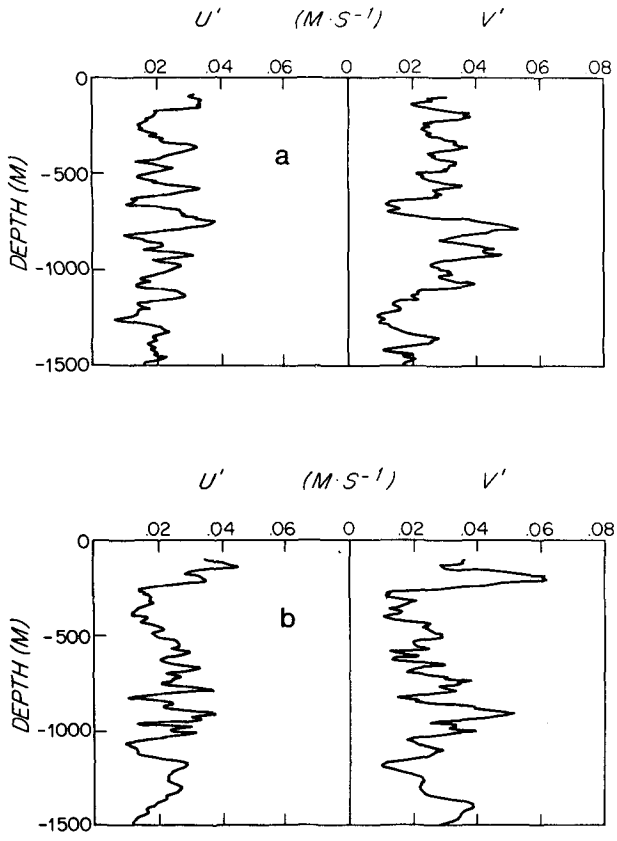

FIG. 5. The rms east (u') and north (v') velocity component differences between data and model for sets 2-5 (a) and 5-8 (b).

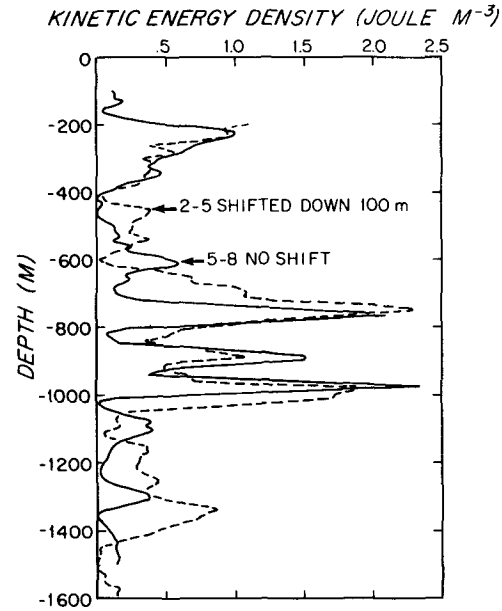

FIG. 6. Profile sof $\frac{1}{2}V_I^2$ with the results of set 2-5 shifted down 100 m compared with the set 3-8 profile.

TABLE 2. Amplitudes and phases of a and b wave components of Eq. (8) for data sets 2-5 and 5-8 calculated over the interval $-500 \geqslant z \geqslant -1000$ m.

Profile series 2-5				
Wavelength (m)	a (m s^{-1})	ϕ^a (deg)	b (m s^{-1})	ϕ^b (deg)
500	0.033	148	0.003	9
250	0.011	168	0.004	302
167	0.015	5	0.007	68
125	0.004	326	0.003	238
100	0.005	225	0.001	324
83	0.001	68	0.002	212
71	0	35	0.002	301
Profile series 5-8				
Wavelength (m)	a (m s^{-1})	ϕ^a (deg)	b (m s^{-1})	ϕ^b (deg)
500	0.021	158	0.008	78
250	0.005	328	0.003	204
167	0.018	69	0.007	172
125	0.010	11	0.009	240
100	0.001	92	0.001	354
83	0.004	41	0.003	209
71	0.001	58	0.001	241

inertial band of the set 2-5 is shifted downward 100 m and plotted with that of the unshifted 5-8 series. Such a shift is consistent with a downward group velocity for the inertial waves.

Although the role of horizontal advection cannot be ignored, its influence cannot be determined with the available data. Since there are no horizontally spaced profiles, the horizontal scales of these features are not known.

The mean time for the sequence 5-8 is 48 h after the mean time for the series 2-5. The apparent 100 m downward propagation of the kinetic energy structure over 2 days yields a vertical group velocity of

$$C_g \approx \frac{-100 \text{ m}}{48 \text{ h}} \approx -0.6 \text{ mm s}^{-1}. \quad (7)$$

Because this estimate of C_g is about equal to that found from the phase analysis, approximate wave theory suggests that waves of 400 m vertical wavelength are primarily responsible for the evolution of the structure of the V_I profiles.

The preceding analysis has indicated that both the phase and amplitude fluctuations are consistent with downward energy propagation. As stated previously, in order to interpret the behavior of current direction with depth it is necessary to isolate the contributions from each vertical wavenumber. In essence, the profiles of V_I and Φ_I must be decomposed into waves propagating energy upward and downward. Estimates of the energies associated with waves with opposite vertical group velocities are obtained using a method of vector spectrum analysis. This method, developed by Gonella (1972) and Mooers (1973) for time series analysis, has recently been applied by Leaman and Sanford (1975) to profiles of internal waves. In the present case we are able to apply the vector analysis selectively to the near inertial-period motions.

The inertial period currents of Eq. (4) can be represented as a Fourier series of vertically propagating waves. Suppressing the common factor $e^{-i\omega t}$, the vertical structure is of the form

$$V_I e^{-i\Phi_I} = A(z) - iB(z)$$
$$= \sum_{j=0}^{M} \{a_j \exp[i(m_j z + \phi_j^a)] + b_j \exp[-i(m_j z - \phi_j^b)]\}, \quad (8)$$

where a_j, b_j are real, positive coefficients, $m_j = 2\pi j/H$, $j = 0, 1, 2, \ldots, M$, the data spacing ΔZ is 10 m, H is depth interval being analyzed, and $M = H/2\Delta Z$. Recalling the factor $e^{-i\omega t}$, it is seen that the vertical phase velocity is positive for the a_j waves and negative for the b_j waves. The corresponding group velocities are of opposite sign.

We let the cosine and sine transforms of $A(z)$ be denoted as A_j^c and A_j^s, where

$$\begin{Bmatrix} A_j^c \\ A_j^s \end{Bmatrix} = \frac{2}{H} \int_{Z-H}^{Z} A(z) \begin{Bmatrix} \cos m_j z \\ \sin m_j z \end{Bmatrix} dz,$$

with an identical definition for B_j^c and B_j^s.

By taking the Fourier transform of Eq. (8) the following relations can be derived:

$$a_j^2 = \tfrac{1}{4}[(A_j^c - B_j^s)^2 + (A_j^s + B_j^c)^2],$$
$$b_j^2 = \tfrac{1}{4}[(A_j^c + B_j^s)^2 + (A_j^s - B_j^c)^2],$$
$$\phi_j^a = \tan^{-1}\left[\frac{-(A_j^s + B_j^c)}{(A_j^c - B_j^s)}\right],$$
$$\phi_j^b = \tan^{-1}\left[\frac{(A_j^s - B_j^c)}{(A_j^c + B_j^s)}\right].$$

The results of the two-wave decomposition, presented in Table 2, reveal that more than four times the energy is propagating downward (the a terms) than upward (the b terms). Most of the energy is contained in the downward going wave of 500 m vertical wavelength. The same analysis over the depth interval from 200 to 1200 m indicates that there is little energy at 1000 m wavelengths, and that again the energy peak is at 500 m, with lesser contributions in the wavelength band 200–500 m.

Thus the rotation with depth evident in Fig. 4 can be ascribed to a dominant downward wave of 500 m,

with weaker variations produced by other downgoing waves of smaller wavelength. Standing waves or modes in the vertical are not present in these data since there is significantly more energy in the downgoing wave. For a standing wave to exist it is necessary that $a_j = b_j$, a condition which is not met for the energetic wave components.

5. The geostrophic balance

Returning to the low-frequency components, we wish to compare U_g and V_g with the geostrophic shear profiles computed from hydrographic station data. Interspersed among the velocity profiler deployments were over 20 STD stations. The geostrophic shear has been computed for the latter half of the stations taken over the same period of time as the profile series 5-8. The earlier STD stations were not used because of obvious depth errors on the analog chart of the STD. This difficulty was resolved prior to the profile series 5-8.

Since the velocity profilers determined that the dominant shear was in the north component, the stations were principally distributed along an east-west oriented line, 20 km in length, centered at the profile site. The dynamic height values were computed relative to 800 m and fitted at selected depths to a two-dimensional surface by a least-square method. The geostrophic shear was computed from the slopes of the dynamic height surfaces.

The results of these computations performed by Richard Scarlet (personal communication) are shown in Fig. 7, together with the mean velocity profile over the same time interval (Fig. 3). About 0.035 m s^{-1} have been added to the relative, geostrophic shear profile to give the best overall agreement. Both the geostrophic computations and direct measurements produced a 0.075 m s^{-1} shear across the thermocline (200–1200 m). Over smaller intervals the data agree quite well, being within 1 standard deviation of the geostrophic shear estimates. It is probably misleading to expect closer agreement than that observed. We suspect that the true mean profile, obtained over a longer series of more closely spaced and more accurate profiles, is in fact smoother than the profile of Fig. 7. That is, we suspect that "mean" shears of as much as 0.05 m s^{-1} over 200 m are not representative of the geostrophic structure However, until more extensive measurements are obtained, the reality of such structure cannot be determined.

6. Summary

We have established that the two velocity profiling techniques reveal the same vertical structure of horizontal motion. This is a most important confirmation of the principle of operation of the electromagnetic velocity profiler. Subsequently, the instrumentation has undergone further development and is now a research tool,

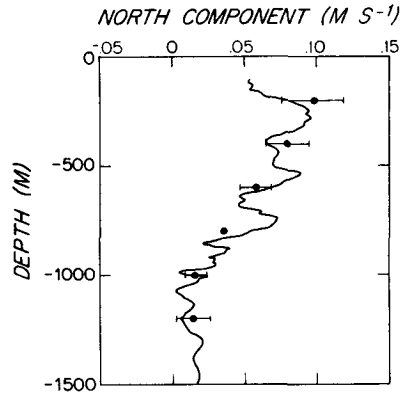

FIG. 7. Comparison of V_g profile from set 5-8 with geostrophic shear profile. Reference level is at 800 m and the error bars represent ±1 standard deviation resulting from fit of density data to two-dimensional plane at other levels.

which is in operational use (Sanford, 1975). Plans are underway to obtain absolute velocity profiles as well.

We have shown in this study that the inertial-frequency-band energy propagates downward at a group velocity of about 0.5 mm s^{-1}. The vertical flux of kinetic energy ($\frac{1}{2}C_g V_I^2$) is as large as 10^{-3} J m^{-2} s^{-1} (1 erg cm^{-2} s^{-1}) in the energetic features of Fig. 6. This net downward energy flux suggests near-surface forcing and little generation or energy reflection at the sea floor. Averaged over the total water column, downward energy flux was observed also by Leaman and Sanford (1975) from data in the same area but at a different time.

Finally, we have demonstrated substantial agreement between the low-pass filtered profile (internal wave energy removed) and the dynamically computed velocity profile from the STD data. The agreement is comparable to that reported by Swallow (1971).

A choice among the three methods discussed depends not only on the availability of the required instruments but also on the constraints imposed by each method. A discussion of the dynamic method need not be presented here, but we do make some remarks about the free-fall profilers. Clearly they are useful in strong currents where current meter moorings cannot be applied. Other applications include the study of internal waves and local dynamical investigations of ocean fronts and processes that are intermittent with respect to depth such as lateral intrusions of different water masses. One distinction between the methods, one which may be of vital importance in some applications, is the amount of data which is available on a near real-time basis. In our experiment the EM data were available as they were obtained while no tracking information was available until long after the experiment. The cost of the instruments and of the data processing are comparable. The principal differences between the profile methods are that the acoustic tracking yields absolute velocity profiles in a restricted

area, i.e., within range of the moored hydrophones, while the electromagnetic method yields relative or shear profiles in virtually any region. Thus, for time series measurements at one location the acoustic method is more suitable for it yields absolute profiles. On the other hand, a survey of the density and relative current fields over a large geographic area is better conducted with the EM method.

A major question that will confront us in surveys of the quasi-geostrophic velocity field is what is the minimum amount of profiling needed in order to determine unambiguously the vertical structure of subinertial motion. We do not have the answer, but there is evidence that under some conditions the geostrophic structure is limited to the barotropic and lowest baroclinic modes (Rossby, 1974; Sanford, 1975).

It would be of great value to understand and to be able to predict under what conditions the geostrophic velocity variance can be obtained by vertical wavenumber filtering (or mode analysis) of individual profiles thereby relaxing the need for repeated sampling in time.

Acknowledgments. We wish to thank Henry Stommel for his help with the STD survey and Richard Scarlet for providing the geostrophic shear computations. John Dunlap digitized and processed the EM profiler data. This research was supported by the Office of Naval Research under Contract N00014-66-C0241 NR 083-004 with the Woods Hole Oceanographic Institution and Contract N00014-67-A-0097-0001 with Yale University.

REFERENCES

Drever, R. G., and T. B. Sanford, 1970: A free-fall electromagnetic current meter instrumentation. *Proc. IERE Conf. Electronic Engineering in Ocean Technology*, Vol. 19, 353–370.

Gonella, J., 1972: A rotary-component method for analyzing meteorological and oceanographic vector time series. *Deep-Sea Res.*, **19**, 833–846.

Leaman, K. D., and T. Sanford, 1975: Vertical energy propagation of inertial waves: A vector spectral analysis of velocity profiles. *J. Geophys. Res.*, **80**, 1975–1978.

Mooers, C. N. K., 1973: A technique for the cross-spectrum analysis of pairs of complex-valued time series, with emphasis on properties of polarized components and rotational invariants. *Deep-Sea Res.*, **20**, 1129–1141.

Munk, W. H., and N. Phillips, 1968: Coherence and band structure of inertical motion in the sea. *Rev. Geophys.*, **6**, 447–472.

Pollard, R. T., 1970: On the generation by winds of inertial waves in the ocean. *Deep-Sea Res.*, **17**, 795–812.

Rossby, H. T., 1969: A vertical profile of currents near Plantagenet Bank. *Deep-Sea Res.*, **16**, 377–385.

——, 1974: Studies of the vertical structure of horizontal currents near Bermuda. *J. Geophys. Res.*, **79**, 1781—1791.

Sanford, T. B., 1971: Motionally-induced electric and magnetic fields in the sea. *J. Geophys. Res.*, **76**, 3476–3492.

——, 1975: Observations of the vertical structure of internal waves. *J. Geophys. Res.*, **80**, 3861–3871.

Siedler, G., 1971: Vertical coherence of short-periodic current variations. *Deep-Sea Res.*, **18**, 179–191.

Swallow, J. C., 1971: The Aries current measurements in the western North Atlantic. *Phil. Trans. Roy. Soc. London*, **A270**, 451–460.

Webster, F., 1972: Estimates of the coherence of ocean currents over vertical distances. *Deep-Sea Res.*, **19**, 35–44.